Interpretation of the Anomalous Transient Behavior in a Heterogeneously Catalyzed Reaction Caused by a Dual Path Way[*]

Atsushi KASAI[**], Boris Golman[***], Tohru KANNO[**] and Masayoshi Kobayashi[**]

(Received May 6, 1993)

Abstract

The complicated transient behavior observed in the oxidation of CO over two differently prepared zinc oxides (K25-ZnO and Kan-ZnO) has been interpreted based on the dual path models. The characteristic transient response curves are classified into four types ; (1) monotonous, (2) overshoot, (3) false start and (4) complex types. The mode is sensitively influenced by the magnitude of CO concentration jump given at the inlet of the reactor. The drastic shift between any two characteristic modes can be visualized as a function of CO-concentration by using a computer simulation technique.

1. INTRODUCTION

In the past seventy years, the kinetic analysis in heterogeneously catalyzed reaction has basically been derived from the Langmuir-Hinshelwood model which was used for the analysis of catalytic kinetic data during the 1920s. In 1943, Hougen and Watson have developed a new kinetic building method based on the Langmuir-Hinshelwood model. They made an attention to adsorption rate control, poisoning, and mass transfer limitations with porous catalysts, as well as the formulation of rate equations for surface-controlled catalytic reactions. In 1950, Yang and Hougen have further developed a simple method to discriminate one reasonable kinetic model between a large number of possible models[1]. All of these models have been thought as a single pathway even though a progress of multi-reaction pathways during steady state conditions because of heterogeneity of solid surface, mobility of metal catalyst particles and easy transfer of adsorbed species between metal catalyst and support.

Tamaru et al.[2] demonstrated that CO oxidation on ZnO was consisted of two pathways : (1) Eley-Rideal (E-R) pathway with an activation energy of 20.7Kcal/mol and (2) Langmuir-Hinshelwood (L-H) pathways with high activation energy. Fiolitakis and Hofmann[3] reported a three-path reaction kinetic model for the water-gas shift reaction on the oxidation state of a CuO/ZnO industrial catalyst. The model consists of two formal Eley-Rideal type mechanisms which are relevant for the microkinetic shift conversion through adsorption intermediates of CO and H_2O, and a redox mechanism which regulates the oxygen activity on the catalyst surface and accounts for the interaction catalyst/reaction medium. Cun-

---

ningham and Hodnett[4] proposed a two parallel photoassisted pathway mechanism to produce hydrogen for the photo-oxidation of secondary alcohol on ZnO and TiO_2, one being L-H and the other E-R in character.   Hori et all[5] showed a dual route model for the N_2O-CO reaction on SnO_2 consisting of a catalyst redox mechanism with N_2O and CO over the catalyst in more reduced states, and a reaction between adsorbed CO and gaseous N_2O.

Weiss and Folman[6] reported a two reaction pathway mechanism for the oxidation of CO on ZnO films on silver.   They are a L-H consisting of the reaction between adsorbed CO and oxygen, and an E-R mechanism consisting of the reaction of gaseous CO with adsorbed oxygen.   The rate equation depends on the thickness of ZnO film on Ag.

Kobayashi et al[7-12] have demonstrated the two path models for CO oxidation on various metal oxides and metals which are controlled by two different active sites and adsorbed species : two different kind of oxygen species (1) one being high oxidation power and the other lower oxidation power on MnO_2[13], Cr_2O_3 and Pb_3O_4, and (2) one being neutral oxygen and the other O^-.   The kinetic analysis of the complex reactions consisting of multi-pathways has some difficulties such as (1) discrimination of each reaction path, (2) classification of elementary steps belonging to the path, (3) recognition of the surface active species for each path and (4) characterization of the transient response curves.   When one can choose a specified concentration region of reactant in which one route is advantage rather than others, transient behavior obtained is strongly influenced by the possible pathway.   The aim of this study is focused on two problems for the multi-pathway reactions : (1) discrimination of the multi-pathways and (2) visualization of the shift of advantage reaction pathway according to gas composition by using the transient response method and CO oxidation on two differently prepared ZnO as a typical model reaction.

2. EXPERIMENTAL

The experimental setup and preliminary investigations are described elsewhere[14,15]. The catalysts were prepared from two different production companies Kanto (Kan-ZnO) and New Jersey Zinc Co. (K25-ZnO).   For Kan-ZnO, metallic zinc is melted, evaporated at 1000°C, oxidized, and cooled.   The fine powder obtained is oxidized again to producing purified ZnO.   For K25-ZnO, a mixture of both zinc carbonate ($ZnCO_3$) and a reductant is heated, evaporated, oxidized in air, and cooled.   And the sample is treated as same as K25-ZnO to produce a high purity of ZnO.   Fig.1 shows scanning electron micrographs of microcrystalline ZnO for the two samples.   The surface of K25-ZnO seems to be fine crystallite particles rather than Kan-ZnO.   They produced two different surface areas $4m^2/g$ for Kan-ZnO and $20m^2/g$ for K25-ZnO.   NEC PC9801DS was used to simulate the transient response curves.   The reactor parameters used in this study are summarized in Table 1.
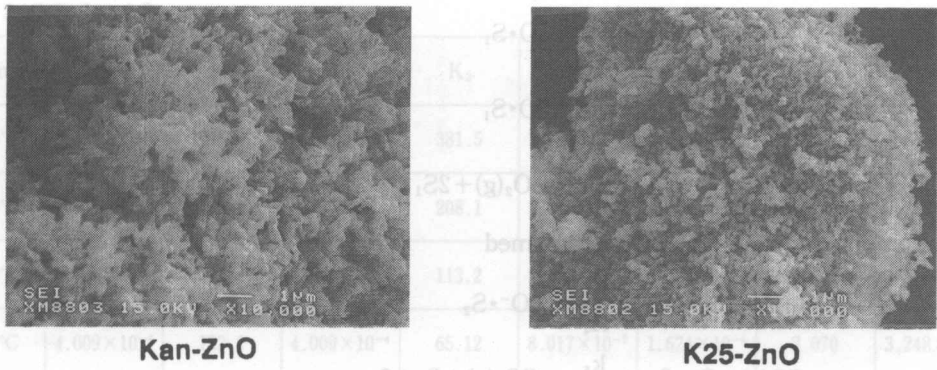
*   The paper was presented at the second Hokkaido regional meeting of the Chemical Engineering Society of Japan
**   Department of Chemical System Engineering
*** Chemical Environmental Engineering

Kan-ZnO   **K25-ZnO**

Fig. 1 Scanning electron micrographs of microcrystalline ZnO

Table 1. Reactor parameters

Catalyst	T	S	W	L	U	S_I	S_{II}	ε	ρ_C
K25-ZnO	130 ~170	20	78.3 (20~40 mesh)	58.7	204	1.1×10^{-6}	1.1×10^{-6}	0.56	1.7
Kan-ZnO	190 ~250	4.0	189.6 (20~40 mesh)	154 (190~225°C) 55.4 (250°C)	221.3	1.6×10^{-6}	2.7×10^{-6}	0.56	1.7

T : Reaction temperature (°C)
S : Catalyst surface area (m²/g)
W : Catalyst weight (g)
L : Reactor length (cm)

U : Superfical gas velocity (cm/min)
S_I, S_{II} : Total amount of active sites (mol/g)
ε : Porosity (−)
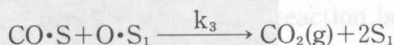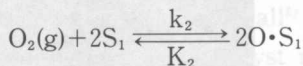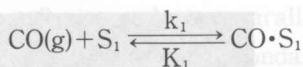ρ_C : Catalyst bed density (g/cm³)

3. Reaction Model

On Kan-ZnO, one can proposed the following two reaction path mechanism based on a large number of steady state and transient state data, for reaction path I in which O^- is an active species
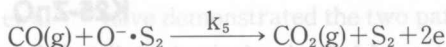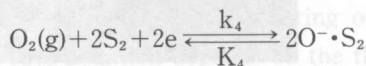
$$CO(g)+O^-\cdot S_I \xrightarrow{k_I} CO_2\cdot S_I +e$$
$$O_2(g)+2S_I +2e \rightleftharpoons 2O^-\cdot S_I$$
$$CO_2\cdot S_I \rightleftharpoons CO_2(g)+S_I$$
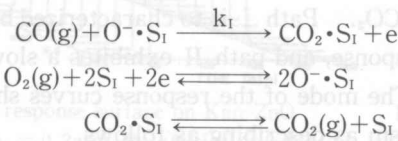
for reaction path II in which a neutral oxygen is an active species

$$CO(g)+O\cdot S_{II} \xrightarrow{k_{II}} CO_2\cdot S_{II}$$
$$O_2(g)+2S_{II} \rightleftharpoons 2O\cdot S_{II}$$
$$CO_2\cdot S_{II} \underset{k_{CO2}}{\overset{k_{IICO2}}{\rightleftharpoons}} CO_2(g)+S_{II}$$
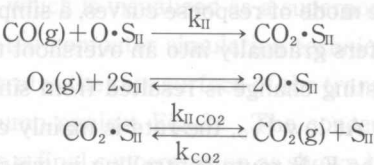
On K25-ZnO, the following model is proposed for reaction path 1 in which neutral oxygen is given

$$CO(g)+S_1 \underset{K_1}{\overset{k_1}{\rightleftharpoons}} CO{\cdot}S_1$$

$$O_2(g)+2S_1 \underset{K_2}{\overset{k_2}{\rightleftharpoons}} 2O{\cdot}S_1$$

$$CO{\cdot}S+O{\cdot}S_1 \overset{k_3}{\longrightarrow} CO_2(g)+2S_1$$

for reaction path 2 in which O^- is assumed

$$O_2(g)+2S_2+2e \underset{K_4}{\overset{k_4}{\rightleftharpoons}} 2O^-{\cdot}S_2$$

$$CO(g)+O^-{\cdot}S_2 \overset{k_5}{\longrightarrow} CO_2(g)+S_2+2e$$

All of k_j and K_j values are represented in Table 2.

It is still unclear why this extraordinary difference of mechanism even though the X-ray diffraction analysis gives same wultzite-type structure of crystalline.　Bolis et al[16] demonstrate that three polycrystalline ZnO samples give different surface activity, and then explain it as the difference in morphology of crystalline.　In our case, one may presume the same idea.　K25-ZnO has more shape edge of crystals and activity for CO-adsorption rather than Kan-ZnO, taking into account the crystal morphology and surface area difference between the two samples.

4. Transient Response Surface

Fig. 2 illustrates the transient response surface caused by the concentration jumps of CO at the inlet of reactor on Kan-ZnO.　The magnitudes of CO concentration jumps are changed in the region from 0.05 to 0.70 atm.　The surface visualizes a monotonous shift from a low to a high rectangular types with increasing P_{CO}.　This simple mode is resulted from the two reaction routes consisting two different Eley-Rideal mechanisms.　In the two, the rate of path I is controlled by the reaction between negatively charged oxygen and gaseous CO forming gaseous CO_2, and the rate of path II is controlled by the reaction of neutral surface oxygen with gaseous CO forming adsorbed CO_2.　Path I is to characterized by the instantaneous change at the initial stage of the response, and path II exhibites a slow monotonous mode at the followed stage of path I.　The mode of the response curves shows a drastic change depending on the reaction mechanism as describing as follows.

Fig. 3 illustrates the transient response surface prepared by the concentration jump of CO on K25-ZnO.　Noting the change of the mode of response curves, a simple instantaneous mode of the low concentration of CO transfers gradually into an overshoot type indicating a steep peak at $P_{CO}=0.70$ atm.　This interesting change is resulted from simultaneous progress of the two different reaction routes.　At low P_{CO}, the rate is mainly controlled by the L-H route and then it shifts gradually to the E-R route controlling in which CO_2 is formed from the E-R route at the initial stage of the response and then the rate is reduced by the L-H route reaching a new steady state level.　This is the reason why the curve exhibits the

Table 2. Calculated Parameters

Temp.	k_1'	K_1	k_2	K_2	k_3	k_4	K_4	k_5
130°C	3.882×10^{-5}	248.6	3.882×10^{-5}	381.5	7.763×10^{-8}	9.240×10^{-6}	105.1	1.848×10^{-8}
140°C	8.075×10^{-5}	197.7	8.075×10^{-5}	208.1	1.615×10^{-7}	2.628×10^{-5}	30.43	5.256×10^{-8}
150°C	1.729×10^{-4}	145.4	1.729×10^{-4}	113.2	3.458×10^{-7}	6.870×10^{-5}	10.08	1.374×10^{-7}
160°C	4.009×10^{-4}	122.2	4.009×10^{-4}	65.12	8.017×10^{-7}	1.624×10^{-4}	3.070	3.248×10^{-7}
170°C	7.500×10^{-4}	103.4	7.500×10^{-4}	34.76	$1,500 \times 10^{-6}$	4.249×10^{-4}	1.137	8.498×10^{-7}

Temp.	k_I	k_{II}	$K_{II\,CO_2}$	K_{CO_2}
190°C	2.6×10^{-7}	3.9×10^{-7}	2.19×10^{-8}	991
200°C	5.0×10^{-7}	5.0×10^{-7}	4.35×10^{-8}	650
225°C	2.1×10^{-6}	6.9×10^{-7}	2.14×10^{-7}	112
250°C	6.6×10^{-6}	1.1×10^{-6}	9.07×10^{-7}	27.5
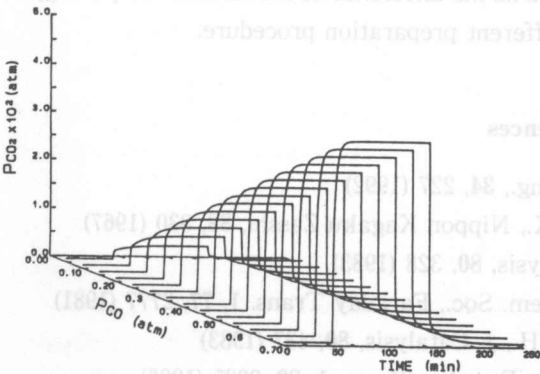
Fig. 2 Transient response surface on Kan-ZnO
Temp. = 225°C, $P_{O_2} = 0.2$atm, P_{CO} (initial) = 0.01atm

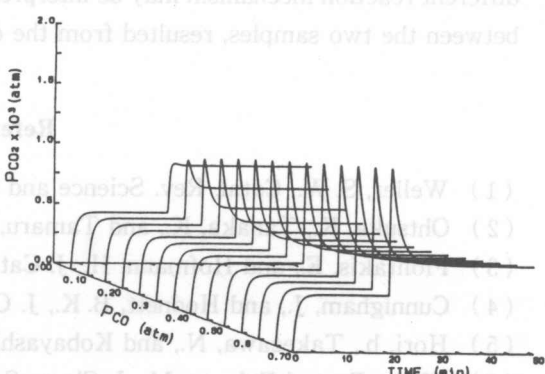**Fig. 3** Transient response surface on K25-ZnO
Temp. = 150°C, $P_{O_2} = 0.2$atm, P_{CO} (initial) = 0.01atm

overshoot type, which is visualized as a superposition of both E-R and L-H routes as shown in Fig. 4 (B) by the computer simulation technique.

Fig. 5 illustrates the rate surface of the transient response curves obtained by the inverse concentration jump against Fig. 3. The concentration of CO is decreased from an initial concentration to a final concentration as shown in the figure. The mode of the curves varies drastically from a monotonous to a complex type. The monotonous mode is due to the L-H route because of its advantage progress at the high concentration of CO. The complex
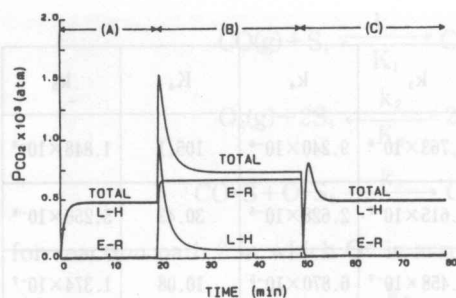
Fig. 4 Transient respose curves on K25-ZnO
Temp. = 150°C, Po_2 = 0.2atm, Pco = 0.01−0.70−0.01atm

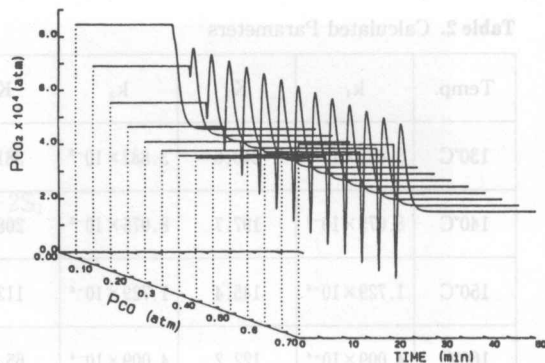**Fig. 5** Transient response surface on K25-ZnO
Temp. = 150°C, Po_2=0.2atm, Pco (final) = 0.01atm

mode is resulted from the comparable progress of the both E-R and L-H routes.   This can be seen from an individual computer simulation of each route as shown in Fig. 4 (C).

5. Conclusions

The transient response surface is visualized on the two differently prepared ZnO (K25 and Kan-ZnO), and the mode of the surface exhibits an extraordinary difference depending on the samples.   On Kan-ZnO, the surface shows a monotonous type in all region of P_{co} and on K25-ZnO shifts from a monotonous to a complicated type depending on P_{co}.   This different reaction mechanism may be interpreted as the difference of the surface morphology between the two samples, resulted from the different preparation procedure.

References

(1) Weller, S. W., Catal. Rev. Science and Eng., **34**, 227 (1992)
(2) Ohtsuka, K., Tanaka, K., and Tamaru, K., Nippon Kagaku Zasshi, **88**, 830 (1967)
(3) Fiolitakis, E., and Hofmann, H., J. Catalysis, **80**, 328 (1983)
(4) Cunnigham, J., and Hodnett, B. K., J. Chem. Soc., Faraday Trans. 1, **77**, 2777 (1981)
(5) Hori, b., Takezawa, N., and Kobayashi, H., J. Catalysis, **80**, 437 (1983)
(6) Weiss, E., and Folman, M., J. Chem. Soc., Faraday Trans. 1, **82**, 2025 (1986)
(7) Kobayashi, M., Kobayashi, H., J. Catal., **27**, 100, 108, 114 (1972)
(8) Kobayashi, M., Kobayashi, H., J. Catal., **35**, 74 (1974)
(9) Kobayashi, M., Kobayashi, H., Bull. Chem. Soc. J., **49** 3009, 3014, 3018 (1976)
(10) Kobayashi, M., "Chemical Reaction Engineering", Ed. J. Wei., C. Georgalsis, ACS, 213 (1982)
(11) Kobayashi, M., Kobayashi, H., Kanno, T., Chem. Eng. Comm., **66**, 23 (1988)
(12) Kobayashi, M., Kanno, T., Kimura, T., J. C. S., Faraday Trans., **84**, 2099 (1988)
(13) Kobayashi, M., Matsumoto, H., Kobayashi, H., J. Catalysis, **21**, 48 (1971)
(14) Hakozaki, M., Golman, B., Kanno, T., and Kobayashi, M., Memoirs of the Kitami

Institute of Technology, **24**, 17, (1992)

(15) Kobayashi, H., Kobayashi, M., Catal. Rev. Science and Eng., **10**, 139 (1974)

(16) Bolis, V., Fubini, B., and Giamello, E., J. Chem. Soc., Faraday Trans. 1, **85**, 855 (1989)